Comparison of Distribution and Toxicity of Different Types of Zinc-Based Nanoparticles

Eun-Jung Park,[1] Uiseok Jeong,[2] Cheolho Yoon,[3] Younghun Kim[2]

[1]Myunggok Eye Research Institute, Konyang University, Daejeon 302-718, Korea

[2]Department of Chemical Engineering, Kwangwoon University, Seoul 139-701, Korea

[3]Seoul Center, Korea Basic Science Institute, Seoul 126-16, Korea

Received 7 March 2016; revised 14 July 2016; accepted 17 July 2016

ABSTRACT: Zinc-based nanoparticles (Zn-NPs), mainly zinc oxide (ZnO) NPs, have promising application in a wide area, but their potential harmful effects on environment and human health have been continuously raised together with their high dissolution rate. In this study, we coated the surface of ZnO NPs with phosphate (ZnP NPs) and sulfide (ZnS NPs) which have very low solubility in water, administered orally (0.5 and 1 mg/kg) to mice for 28 days, and then compared their biodistribution and toxicity. As expected, ZnO NPs were rapidly ionized in an artificial gastric fluid. On the other hand, ZnO NPs were more particlized in an artificial intestinal fluid than ZnP and ZnS NPs. After repeated dosing, all three types of Zn-NPs the most distributed in the spleen and thymus and altered the level of redox reaction-related metal ions in the tissues. We also found that three types of Zn-NPs clearly disturb tissue ion homeostasis and influence immune regulation function. However, there were no remarkable difference in distribution and toxicity following repeated exposure of three types of Zn-NPs, although $Na+$ and $K+$ level in the spleen and thymus were notably higher in mice exposed to ZnO NPs compared to ZnP and ZnS NPs. Taken together, we suggest that all three types of Zn-NPs may influence human health by disrupting homeostasis of trace elements and ions in the tissues. In addition, the surface transformation of ZnO NPs with phosphate and sulfide may not attenuate toxicity due to the higher particlization rate of ZnO NPs in the intestine, at least in part. © 2016 Wiley Periodicals, Inc. Environ Toxicol 32: 1363–1374, 2017.

Keywords: zinc oxide nanoparticles; transformation; redox reaction; ion homeostasis; immune response

INTRODUCTION

Zinc (Zn)-based nanoparticles (Zn-NPs), mainly zinc oxide (ZnO) NPs, have been widely used as a raw material for consumer products, such as cosmetics and paints, due to their efficient ultra violet (UV) blocking and anti-bacterial properties, as well as their low toxicity and high skin tolerance. Additionally, Zn-NPs have been used in electronic devices due to its super hydrophobic and photo-catalytic properties. Akhtar et al. (2012) also raised the potential of ZnO NPs as anticancer drugs due to their selective induction of apoptotic cell death in cancer cells, but not normal cells. On the other hand, some researchers indicated the possible hazardous effects of ZnO NPs exposed to the environment and human health in the production, usage, and disposal process (Vandebriel and De Jong, 2012; Nohynek et al., 2010). For example, ZnO NPs (2.5 g/kg) distributed in the liver, spleen, lung, and kidney after oral administration and caused the transient histopathology in the liver (Li et al., 2012). ZnO NPs instilled intratracheally also increased LDH release, BAL

Additional Supporting Information may be found in the online version of this article.

Correspondence to: Dr. E.-J. Park; e-mail: pejtoxic@hanmail.net

Contract grant sponsor: Basic Science Research Program through the National Research Foundation of Korea funded by the Ministry of Education, Science and Technology.

Contract grant number: 2011-35B-E00011.

Published online 11 August 2016 in Wiley Online Library (wileyonlinelibrary.com). DOI: 10.1002/tox.22330

cell number, and neutrophil content that was associated with enhanced cytotoxicity (Sayes et al., 2007). Further, ZnO NPs caused severe injury to the alveolar epithelial cells through mitochondrial dysfunction and an increase of intracellular reactive oxygen species (ROS) (Kim et al., 2010).

Accumulating evidences suggest that dissolution is a key factor in determining the biological and toxicological effects of some metal-based NPs, including silver, Zn, and cobalt, and that the dissolution rate (toxicity) depend on particle size and coating materials (Choi and Choy, 2014; Jiang et al, 2015; Kwok et al., 2016). For example, ZnO NPs-induced cytotoxicity was partially mediated by free Zn ions released from ZnO NPs (Kim et al., 2010; Sensi and Jeng, 2004). Additionally, when compared toxicity of cobalt NPs in six different types of cells, the toxic effects were closely related to the dissolution of cobalt ions from the cobalt NPs (Horev-Azaria et al., 2011). Similarly, Zn ion level in the supernatant of cells treated with ZnO NPs significantly correlated with reduced cell viability and increased LDH release (Song et al., 2010). Wang et al (2014) also reported that smaller polyvinylpyrrolidone (PVP)- and citrate-coated silver NPs (20 nm) induced more toxicity and oxidative stress than their larger particles (110 nm) in human bronchial epithelial cells due to the higher dissolution rate and silver bioavailability. As well, smaller citrate-coated silver NPs showed a higher potential to generate acute inflammatory responses in the lungs and to produce chemokines compared to the lager one. Moreover, PVP-coated silver NPs induced less cytotoxic effects than citrated-coated silver NPs, likely due to the ability of PVP to complex released silver ions. According to the previous reports, Zn sulfide (ZnS) and Zn3(PO4)2 particles have very low solubility in water phase (Ma et al., 2013; Rathnayake et al., 2014). Herein, we can expect that surface transformation of soluble Zn particles into insoluble Zn particles may reduce Zn ion release from ZnO NPs, ultimately leading to lower toxicity. Thus, we coated ZnO NPs with phosphate and sulfide, administered three types of Zn-NPs (0.5 and 1 mg/kg) orally for 28 days to mice according to the OECD test guideline 407, and then compared their biodistribution and toxicity.

ABBREVIATIONS

APC	Allophycocyanin
CD	Cluster of differentiation
DW	Drinking water
FITC	Fluorescein isothiocyanate
HDD	Hydrodynamic diameter
IACUC	Institutional Animal Care and Use Committee
ICP-MS	Inductively coupled plasma mass spectrometry
PE	Phycoerythrin
PVP	Polyvinylpyrrolidone
ROS	Reactive oxygen species
UV	Ultra violet

MATERIALS AND METHODS

Preparation and Characterization of Zn-NPs

ZnO NPs (50 wt % in H2O) were purchased from Sigma-Aldrich, and Zn3(PO4)2 NPs (hereafter, ZnP NPs) and ZnS NPs were synthesized by shell-coating ZnO NPs with sodium hydrogen phosphate (Na2HPO4, 99 wt %, Duksan, Gyeonggi-do, Korea) and sodium sulfide hydrate (Na2S, 60 wt %, Duksan). Briefly, ZnO NPs solution was diluted in sterilized drinking water (DW, 100 mL), and Na2HPO4 (40 mg) and Na2S (75 mg) were added to the solution. After 4 h of stirring, the precipitated ZnP and ZnS NPs were separated by ultra-centrifugation, washed 2 times with water, and then re-dispersed in DW (100 μg/mL). The concentration of Zn in the dispersed solution was determined by inductively coupled plasma optical emission spectroscopy (ICP-OES, Optima 2000DV, PerkinElmer, MA, USA), and the morphology, dispersion degree, and particle stability of the three types of Zn-NPs were analyzed by transmission electron microscopy (TEM, JEM-2010, JEOL Ltd., Toyko, Japan). Additionally, hydrodynamic diameter (HDD) and zeta potential were measured with a zeta potential & particle size analyzer (ELS-Z, Otsuka Pharmaceutical Co., Toyko, JAPAN). The three types of Zn-NPs were made freshly every third day to minimize toxic effects by dissolution and aggregation in DW.

Ionization Measurement

The three types of Zn-NPs solution (2 mL) were diluted in artificial gastric fluid (pH 2, 48 mL, Marques et al., 2011) and maintained for 24 h at 37°C. A part of the solution was transferred to another tube and centrifuged at 15,000 rpm for 10 min, and then the supernatant (ionized Zn + 2 solution) was transferred into the artificial intestinal fluid (pH 6.8). After stirring for 30 min, the aggregated or reduced Zn particles were separated by centrifugation (15,000 rpm for 10 min). The ionization level of the three types of Zn-NPs in gastric fluid was measured by ICP-OES (Optima 2000DV, PerkinElmer) and the degree of particlization in the intestinal fluid was calculated with the level of ionization.

Housing and Zn-NPs Treatment

Obtained specific pathogen-free-ICR mice (27–28 g, 6-weeks, male, OrientBio, Seongnam, Gyeonggi-do, Korea) were housed in our pathogen-free facility (23[± 3°C], a relative humidity of 50% [± 10%], a 12-h light/dark cycle with a light intensity of 150–300 Lux, and air circulation of 10–20 times/h) for 1 week before the initiation of the experiment. Diet and water were provided ad libitum. Considering that the upper limit volume of 10 mL/kg is recommended for oral dosing in terms of animal welfare, we dosed orally (0.5 and 1 mg/kg, 5 mice/group) to mice with three types of Zn-NPs (100 μg/mL) for 28 days. The control group was

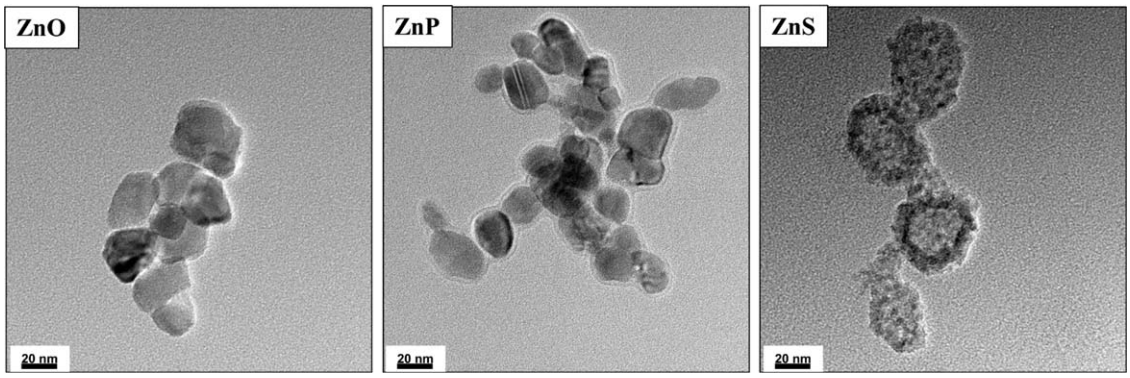

Fig. 1. TEM images of three types of Zn-NPs.

treated with sterilized DW, and body weight was checked weekly. The experiments (IACUC No. 2014-0036) were assessed by the Institutional Animal Care and Use Committee (IACUC) of Ajou University (Suwon, Korea) and performed in accordance with the ILAR publication, "Guide for the Care and Use of Laboratory Animals."

In Vivo Sample Preparation and Blood Analysis

Blood was taken up via the caudal vena cava under carbon dioxide gas euthanization, and a part of the whole blood was centrifuged at 3,000 rpm for 10 min to obtain serum for biochemical analysis. Hematological and biochemical analysis were performed in Neodin Veterinary Science Institute (Seoul, Korea) using a blood autoanalyzer (HemaVet850, CDC Technologies, Inc., Dayton, Ohio, USA) and chemistry analyzer (BS-400, Mindray, Shenzhen, China), respectively. Tissues (brain, thymus, lung, heart, liver, spleen, kidney, and testes) were also collected for further study.

Trace Elements and Ion Concentration Measurement

Tissues and blood were digested in a mixture of HNO3 (70%) and H2O2 (35%) solution using a microwave digestion system (Milestone, Sorisole, Italy) under high temperature (120°C, 8 min; 50°C, 2 min; 180°C, 10 min) and high pressure. Finally, element concentrations and ion level in the lysates were measured according to standard operating procedure using inductively coupled plasma mass spectrometry (ICP-MS) at the Korean Basic Science Institute (Supple 2A) and ICP-OES (OPTIMA 5300DV, Perkin Elmer, USA) at Center for Materials Characterization and Machining, Ajou University (Supple 2B), respectively.

Immunophenotyping Analysis

Splenocytes (5 mice/group) were isolated from the spleen. Briefly, the spleen was ground in RPMI media containing fetal bovine serum (2%). After removing red cells with FACS lysis buffer, the splenocytes were filtered using a 70 μm-pore size nylonmesh, and then resuspended in FACS buffer. After blocking with Fc-block antibody [cluster of differentiation (CD)16/CD32, eBiosciences, San Diego, CA, USA] to reduce nonspecific binding, splenocytes were incubated with the fluorescence dye-labeled antibodies: phycoerythrin (PE)-conjugated anti-CD11b, fluorescein isothiocyanate (FITC)-conjugated anti-CD11c, FITC-conjugated anti-CD3, PE-conjugated anti-CD19, allophycocyanin (APC)-conjugated anti-DX5, PE-conjugated anti-CD4, FITC-conjugated anti-CD8, and FITC-conjugated anti-CD80 (B7-1) (eBioscience), and APC-conjugated anti-CD86 (B7-2, BioLegend, Inc. San Diego, CA, USA) for 30 min at 4°C according to the manufacturer's instructions. Then, cells were washed twice with FACS buffer and analyzed on a FACSCalibur (BD Biosciences) flow cytometer with CellQuest software.

Statistical Analysis

Statistical significance between Zn-NPs-dosed groups and the control group was performed using Student's *t*-test

TABLE I. A summary of physicochemical characterization of Zn-NPs. Zn-NPs were characterized in DW and artificial body fluids (Marques et al., 2011), and each value is mean ± SD of three independent measurement.

		HDD (nm)	Surface charge (mV)
ZnO	DW	87.8 ± 55.8	−16.9 ± 0.3
	Gastric fluid	1415.4 ± 598.8	0.5 ± 0.6
	Intestinal fluid	36.9 ± 2.5	−11.9 ± 1.4
	FBS	155.9 ± 3.2	−8.5 ± 0.3
ZnP	DW	56.8 ± 2.8	−20.8 ± 1.5
	Gastric fluid	1242.3 ± 93.5	0.01 ± 0.9
	Intestinal fluid	44.6 ± 5.9	−12.32 ± 0.5
	FBS	85.2 ± 20.5	−4.69 ± 1.0
ZnS	DW	57.9 ± 3.4	−35.9 ± 0.1
	Gastric fluid	2110.3 ± 305.2	4.8 ± 0.8
	Intestinal fluid	91.3 ± 2.0	−23.8 ± 0.2
	FBS	93.6 ± 25.6	−12.0 ± 1.0

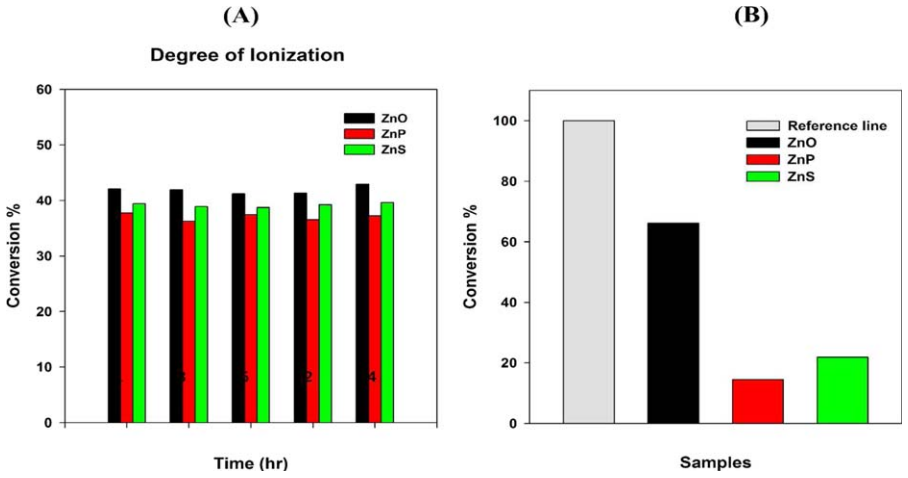

Fig. 2. Chemical behaviors of Zn-NPs in artificial body fluids. (A) Ionization degree in gastric fluid, (B) Particlization degree in intestinal fluid. [Color figure can be viewed at wileyonlinelibrary.com.]

(Graphpad Software, San Diego, CA, USA) or one-way ANOVA test followed by Tukey's post-hoc pairwise comparison. Asterisks (*$p < 0.05$ and **$p < 0.01$) indicate statistically significant differences compared to the control group.

RESULTS

Characterization of Three Types of Zn-NPs

The morphology of ZnO NPs was modified by chemical treatments (i.e., phosphate and sulfide treatment, Fig. 1). Namely, while unmodified ZnO NPs showed some aggregated form of primary particles with ca. 50 nm, ZnP NPs showed a 5 nm sized transparent shell on the surface of ZnO NPs. In addition, ZnS NPs showed an aggregated form of the smaller spherical particles. Meanwhile, HDD of all three types of Zn-NPs indicated the larger values in an artificial gastric fluid compared to them in DW due to decrease of the stability following change of pH (Table I, Greenwood, 2003).

Fate of Zn-NPs in the Body Fluid

Even though the phosphate (ZnP NPs) and sulfide forms (ZnS NPs) of ZnO, are known to have very low solubility in water phase (Ma et al., 2013; Rathnayake et al., 2014), these particles could also be partially ionized in solutions with very low pH (i.e. gastric fluid) (Kim et al., 2004). Therefore, the degree of ionization in the gastric fluid and particlization in the intestinal fluid was evaluated for all three types of Zn-NPs. The ionization ratio of three types of Zn-NPs in gastric fluid (pH 2) was not changed with time, and the ionized level (conversion yield of Zn2+ from NPs) was slightly different by types of Zn-NPs (ZnO > ZnP > ZnS, about $40 \pm 3\%$ regardless of the types of Zn-NPs, Fig. 2A). Meanwhile, in the intestinal fluid, Zn particles reformed from the ionic solution of ZnO NPs was ca. 65%, but those from ionic solution of ZnS and ZnP NPs were under 20% (Fig. 2B).

Changes in Body Weight Following Exposure to Zn-NPs

As shown in Figure 3, when administered for 28 days, an increase in body weight of mice was lower in all the treated groups compared to the control group, and the degree was similar between types of Zn-NPs. At a 1 mg/kg dose, the average body weight gain was 5.9, 6.2, and 6.2 g in the ZnO,

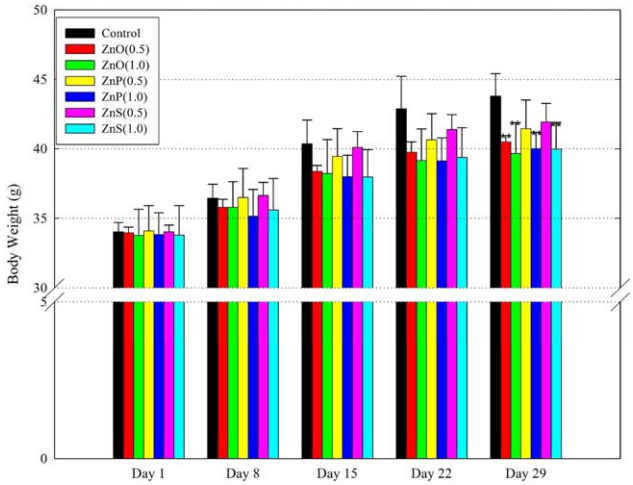

Fig. 3. Changes in body weight following exposure to Zn-NPs. Body weight (5 mice/group) was measured weekly for 4 weeks from dosing, and data are mean ± standard deviation (SD) of each group. Statistical significance in body weight of the treated-groups compared to the control group was evaluated with the body weight gain of mice in each group during the experimental period. *$p < 0.05$, **$p < 0.01$. [Color figure can be viewed at wileyonlinelibrary.com.]

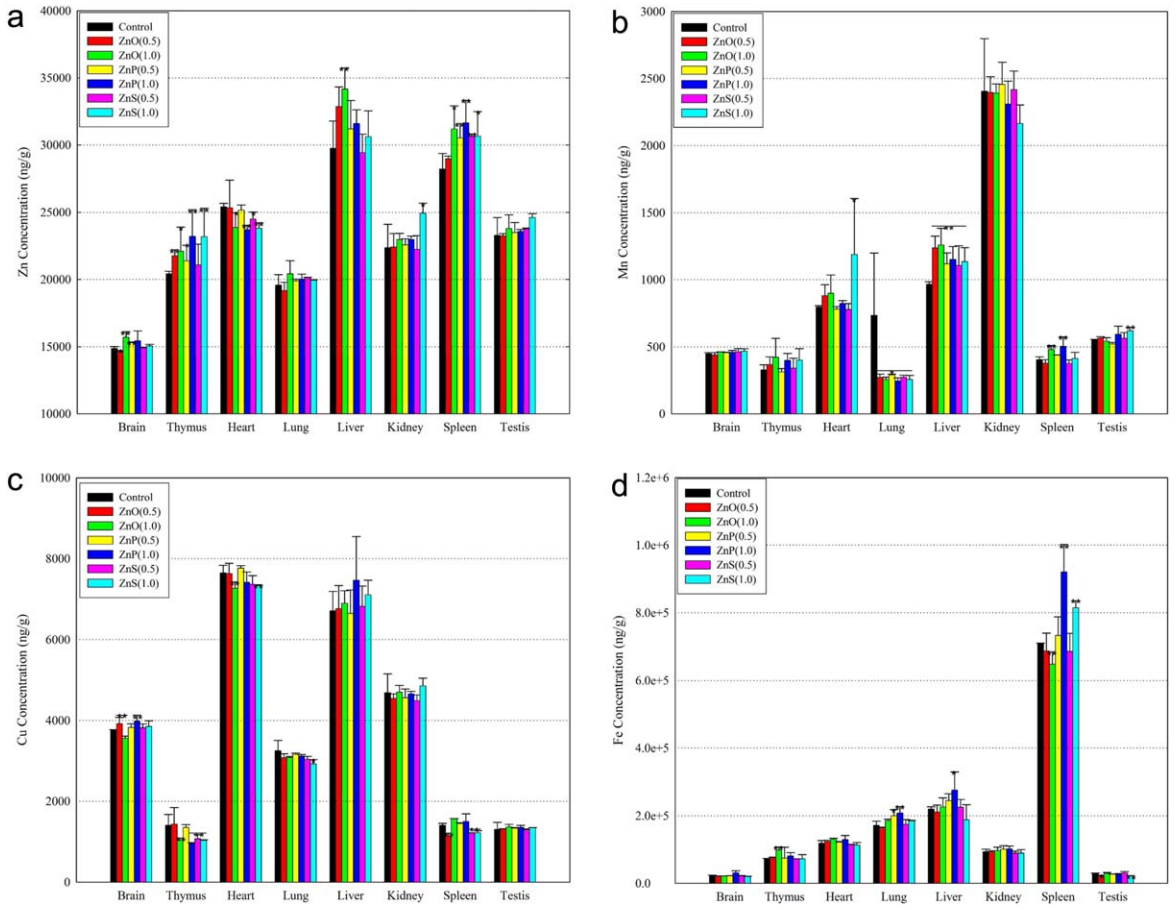

Fig. 4. Tissue level of redox reaction-related trace elements. Each tissue was harvested from mice (5 mice/group) after oral dosing for 28 days (1 time/day), and the level of elements in each sample was measured using ICP/MS according to the suggested analytic condition (Supporting Information Table I). Results represent mean ± SD.*$p < 0.05$, **$p < 0.01$. (A) Zinc (Zn), (B) Manganese (Mn), (C) Copper (Cu), and (D) Iron (Fe). [Color figure can be viewed at wileyonlinelibrary.com.]

ZnP, and ZnS NPs-treated mice, respectively, whereas that was 9.8 g in the control mice (Supporting Information Fig. S1).

Comparison of Zn Level in Tissues of Mice

As compared to the control group, the significant increase in the Zn level following exposure to Zn-NPs was observed in the thymus and the spleen of all the treated-groups exposed at the higher dose (1 mg/kg), as well as in the brain and liver of mice treated with the higher dose of ZnO NPs]Fig. 4(A)]. On the other hand, Zn level in the heart was lower in mice treated with the higher dose of all three types of Zn-NPs compared to the control. Meanwhile, Zn level in the blood did not show any significant changes following administration of Zn-NPs (data not shown).

Alteration of Redox Reaction-Related Trace Element Level in Tissues

In order to compare the effect of three types of Zn-NPs on tissue homeostasis of redox reaction-related trace elements, we measured manganese (Mn), copper (Cu), and iron (Fe) level in each of the tissue samples. When administered at a 1 mg/kg dose, Mn level significantly increased in the liver of all three types of Zn-NPs-treated mice, in the spleen of ZnO and ZnP NPs-treated mice, and in the testis of ZnS NPs-treated mice compared to the control [Fig. 4(B)]. Cu level was clearly reduced in the thymus and lungs of mice exposed to the higher dose of all three types of Zn-NPs, and in the heart and spleen of mice exposed to higher dose of ZnO and ZnS NPs [Fig. 4(C)]. In addition, when administered at a 1 mg/kg dose, remarkable enhance of Fe level was observed in the thymus of mice treated with ZnO NPs, in the lung of mice treated with ZnP NPs, and in the spleen of mice treated with ZnP and ZnS NPs [Fig. 4(D)].

Alteration of Ion Homeostasis Following Exposure to Zn-NPs

In comparison of the control and the higher dose of the treated-groups, the sodium ion ($Na+$) level notably

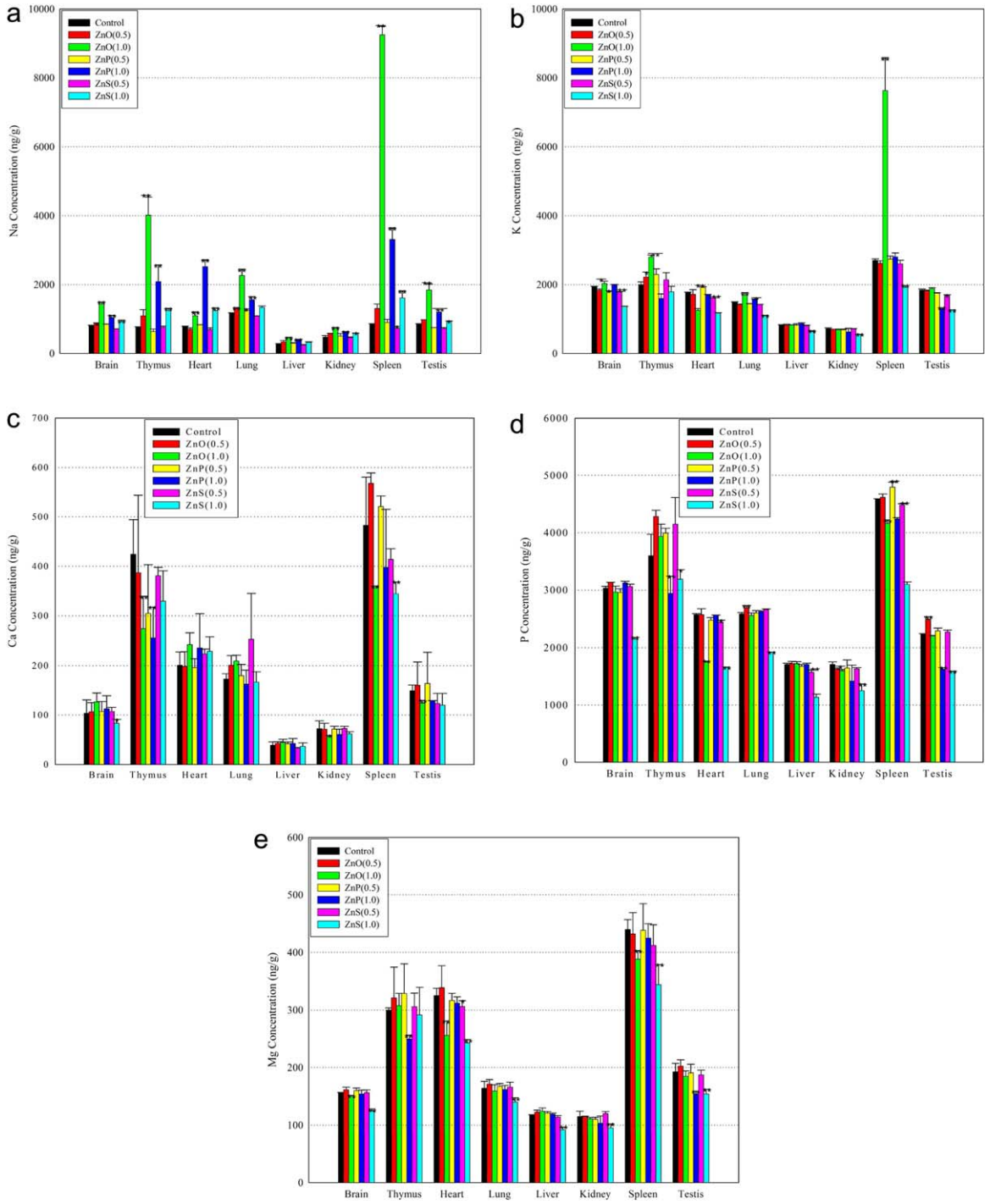

Fig. 5. Effects of Zn-NPs on ion-homeostasis. Ion level in each sample was measured using ICP/OES according to the suggested analytic condition (Supporting Information Table II). Results represent mean ± SD.*$p < 0.05$; **$p < 0.01$.**$p < 0.01$. (A) Sodium (Na+), (B) Potassium (K+), (C) Calcium (Ca2+), (D) Phosphorus (P), and (E) Magnesium (Mg). [Color figure can be viewed at wileyonlinelibrary.com.]

increased in all tissues following exposure to three types of Zn-NPs, and the increased level was generally order of ZnO > ZnP > ZnS NPs [Fig. 5(A)]. Potassium ion (K+) level was elevated in the brain, thymus, lung, and spleen in mice treated with ZnO NPs, whereas it clearly decreased in the heart of mice treated with ZnO NPs, in the thymus and testis of mice treated with ZnP NPs, and in all the tissues in mice treated with ZnS NPs [Fig. 5(B)]. Additionally, calcium ion (Ca2+) level significantly decreased in the thymus and testis of mice treated with all three types of Zn-NPs, in

TABLE II. Biochemical changes following exposure to Zn-NPs. A part of whole blood (5 mice/group) was centrifuged for 10 min at 3,000 rpm

Unit	TP g/dL	Albumin g/dL	Tbil mg/dL	Glucose mg/dL	BUN mg/dL	Cre mg/dL	AST U/L	ALT U/L	ALP U/L	γ-GTP U/L	Amylase U/L	Globulin g/dL	Sodium mmol/L	Potassium mmol/L	Chloride mmol/L
Control	6.1 ± 0.1	3.5 ± 0.0	0.2 ± 0.0	288.7 ± 18.0	21.9 ± 0.7	0.2 ± 0.0	68.7 ± 8.0	31.0 ± 0.8	74.3 ± 16.1	0.0 ± 0.0	3343.5 ± 402.0	2.6 ± 0.1	157.3 ± 1.7	5.9 ± 0.4	118.0 ± 2.2
ZnO (0.5mg/kg)	6.0 ± 0.3	3.5 ± 0.1	0.1 ± 0.0	266.7 ± 18.4	21.1 ± 0.9	0.2 ± 0.0	60.7 ± 11.5	29.7 ± 6.9	83.3 ± 17.9	0.0 ± 0.0	3058.1 ± 210.8	2.5 ± 0.2	159.0 ± 1.6	5.5 ± 0.7	114.8 ± 0.8
ZnO (1.0mg/kg)	5.8 ± 0.3	3.3 ± 0.1	0.2 ± 0.0	237.3 ± 20.6*	23.4 ± 1.9	0.2 ± 0.1	49.0 ± 10.3*	23.8 ± 4.3*	68.8 ± 12.9	0.0 ± 0.0	3166.6 ± 237.4	2.5 ± 0.3	157.2 ± 0.9	6.9 ± 1.1	115.6 ± 1.5
ZnP (0.5mg/kg)	6.2 ± 0.2	3.6 ± 0.1	0.2 ± 0.0	239.3 ± 37.6	20.1 ± 1.3	0.2 ± 0.1	96.7 ± 60.3	33.7 ± 13.1	76.7 ± 16.7	0.0 ± 0.0	3263.0 ± 158.7	2.6 ± 0.2	158.8 ± 3.6	6.5 ± 0.9	116.0 ± 4.0
ZnP (1.0mg/kg)	6.0 ± 0.3	3.4 ± 0.2	0.2 ± 0.0	258.0 ± 7.3*	24.3 ± 1.1	0.2 ± 0.0	71.0 ± 7.8	41.7 ± 11.8	83.0 ± 10.0	0.0 ± 0.0	3497.1 ± 364.9	2.6 ± 0.1	163.3 ± 3.8	5.4 ± 0.3	120.6 ± 4.9
ZnS (0.5mg/kg)	5.3 ± 0.2*	3.2 ± 0.1	0.1 ± 0.0	248.8 ± 23.4	20.4 ± 3.6	0.2 ± 0.1	125.8 ± 51.2	79.5 ± 47.3	64.5 ± 7.1	0.0 ± 0.0	2806.1 ± 188.3	2.1 ± 0.1*	157.5 ± 0.9	5.0 ± 0.3*	115.9 ± 1.3
ZnS (1.0mg/kg)	5.3 ± 0.1*	3.3 ± 0.0	0.1 ± 0.0	279.5 ± 11.9	21.0 ± 2.4	0.2 ± 0.0	81.5 ± 17.0	48.5 ± 6.3*	77.5 ± 12.1	0.0 ± 0.0	2853.7 ± 312.4	2.0 ± 0.1*	157.4 ± 1.2	4.8 ± 0.5*	115.0 ± 1.6

*$p < 0.05$.

TP; Total protein, Tbil; Total bilirubin, Cr; Creatinine, AST; Aspartate aminotransferase, ALT; Alanine aminotransferase, ALP; Alkaline phosphatase, γ-GTP; Gamma-glutamyl transferase.

TABLE III. Hematological changes following exposure to Zn-NPs. Blood was collected from five mice per group ($n = 5$) after oral dosing for 28 days

Unit	WBC K/uL	LY %	MO %	NE %	EO %	BA %	RBC M/mm3	MCV fl	HCT %	MCH pg	MCHC g/dL	Hgb g/dL	RDW %	PLT K/uL	MPV fL
Control	1.5 ± 0.8	79.6 ± 4.2	3.5 ± 3.0	12.8 ± 5.6	2.8 ± 1.6	0.8 ± 0.3	8.0 ± 0.6	49.5 ± 1.3	39.9 ± 3.9	17.7 ± 0.5	35.7 ± 1.4	14.2 ± 1.3	18.1 ± 0.3	891.6 ± 185.4	8.8 ± 1.7
ZnO (0.5mg/kg)	1.4 ± 1.0	63.0 ± 28.0	4.2 ± 3.4	15.4 ± 5.3	2.0 ± 1.0	1.3 ± 0.8	8.2 ± 0.6	47.9 ± 1.0	39.2 ± 2.8	15.3 ± 3.5	31.1 ± 8.5	12.4 ± 2.9	18.4 ± 0.4	925.0 ± 256.0	9.4 ± 1.5
ZnO (1.0mg/kg)	1.6 ± 1.1	75.2 ± 6.3	3.0 ± 2.3	18.3 ± 5.8	2.3 ± 1.5	1.1 ± 0.5	8.8 ± 0.5	48.8 ± 0.8	43.0 ± 3.1	17.1 ± 0.4	35.2 ± 1.2	15.1 ± 0.9	18.2 ± 0.1	923.0 ± 195.9	9.3 ± 0.8
ZnP (0.5mg/kg)	2.3 ± 0.3	83.7 ± 7.3	6.1 ± 4.1	8.0 ± 3.2	0.5 ± 0.5	1.1 ± 0.5	8.9 ± 0.5	49.1 ± 1.0	43.6 ± 1.9	21.0 ± 7.6	31.4 ± 7.9	15.5 ± 0.7	18.3 ± 0.6	902.6 ± 173.3	8.6 ± 1.2
ZnP (1.0mg/kg)	1.5 ± 0.5	74.0 ± 8.2	6.4 ± 4.3	16.8 ± 6.2	1.6 ± 1.3	1.0 ± 0.5	9.0 ± 0.3	40.0 ± 15.5	44.7 ± 3.6	23.0 ± 12.1	31.7 ± 7.8	18.8 ± 6.9	17.9 ± 1.4	728.6 ± 203.9	10.3 ± 0.9
ZnS (0.5mg/kg)	2.1 ± 1.0	80.9 ± 6.0	3.6 ± 4.0	12.4 ± 2.9	2.3 ± 1.3	0.6 ± 0.7	7.7 ± 0.4	49.8 ± 1.6	38.4 ± 2.2	17.6 ± 0.4	35.3 ± 1.3	13.5 ± 0.8	17.7 ± 0.5	937.0 ± 118.7	7.9 ± 0.7
ZnS (1.0mg/kg)	1.9 ± 0.7	79.9 ± 2.7	4.9 ± 3.7	11.4 ± 3.2	3.0 ± 2.9	0.9 ± 0.5	7.7 ± 0.6	49.0 ± 1.0	37.9 ± 3.6	17.1 ± 0.3	34.8 ± 0.6	13.2 ± 1.0	18.3 ± 0.3	900.0 ± 118.1	7.9 ± 0.6

Results represent mean ± SD.

*$p < 0.05$, **$p < 0.01$.

WBC, white blood cells; LY, lymphocytes; MO, monocytes; NE, neutrophils; EO, eosinophils; BA, basophils; RBC, red blood cells; MCV, mean corpuscular volume; HCT, hematocrit; MCH, mean corpuscular hemoglobin; MCHC, mean corpuscular hemoglobin concentration; Hgb, hemoglobin; RDW, red blood cell distribution width; PLT, platelet; MPV, mean platelet volume.

the kidney and spleen of mice treated with ZnO NPs, and in the brain, kidney and spleen of mice treated with ZnS NPs [Fig. 5(C)]. On the other hand, Ca2+ level was significantly elevated in the heart and lung of mice exposed to ZnO NPs. The level of phosphorus ion (P) and magnesium ion (Mg) remarkably decreased in all the tissues, except the thymus, of ZnS NPs-treated mice [Fig. 5(D,E)]. P level was also significantly reduced in the heart, kidney, and spleen of ZnO NPs-treated mice, and in the thymus, spleen, and testis of ZnP NPs-treated mice. Additionally, compared to control, the Mg level was notably lower in the brain, heart, and spleen of ZnO NPs-treated mice and in the thymus and testis of ZnP NPs-treated mice.

Blood Biochemical Changes Following Exposure to Zn-NPs

As shown in Table II, when administered at the higher dose (1 mg/kg), the levels of total protein and globulin significantly decreased in the blood of mice exposed to ZnS NPs compared to the control, whereas the glucose level was lower in mice treated with ZnO and ZnP NPs. As compared to control, ZnO NPs (1 mg/kg) decreased AST and ALT levels, whereas ZnS NPs increased ALT level. Additionally, the K+ level in the blood was significantly reduced in mice treated with ZnS NPs compared to the control. Meanwhile, there were no significant hematological changes following exposure to three types of Zn-NPs (Table III).

Systemic Immunotoxic Response Following Exposure to Zn-NPs

Compared to control, all three types of Zn-NPs decreased the expression of CD86 and CD80 proteins, representative antigen presentation-related markers, on the splenocytes [Fig. 6(A)]. Additionally, maturation of dendritic cells, a representative antigen-presenting cell, was inhibited in mice treated with ZnP and ZnS NPs [Fig. 6(A)]. When compared to the control, while expression of CXCR2 protein, a chemotaxis-related surface marker, was notably reduced in mice exposed to ZnO and ZnS NPs, it was enhanced in mice exposed to ZnP NPs [Fig. 6(B)]. In addition, T cell distribution in lymphocytes increased following exposure to all three types of Zn-NPs, and the increased level was order of ZnO > ZnS >ZnP NPs [Fig. 6(C)].

DISCUSSION

The interactions of NPs with biological systems are key factors in considering the potential toxicity of NPs to human health. Accumulated reports suggest that some metal-based NPs, including silver, cobalt, and Zn, induce harmful health effects via the unique toxic mechanism, which is expressed as "Trojan-horse type mechanism" (Park et al., 2010; Ortega et al., 2014; Sabella et al., 2014). Additionally, it is known that metal-based NPs are generally produced from ionic solutions, thus they can be readily dissolved under conditions of low pH, which ultimately leading to higher toxicity. Thus, engineers have attempted to lower dissolution rate by coating the surface of these NPs (Luo et al., 2014; Wang et al., 2014). Meanwhile, in recent, Kwok et al (2016) reported that dissolution rate of silver NPs largely depended on particle size but their aggregation behavior and toxicity were more determined by coating materials. Additionally, size of cadmium containing quantum dots was more important than the ionized cadmium in inducing toxicity (Zhang et al., 2016). The previous reports suggested that the solubility of ZnS and ZnP NPs is very low (Ksp = 10 − 24 and 10 − 33, respectively), thus the surface transformation of ZnO into ZnP and ZnS may successfully reduce Zn2+ release from ZnO (Ma et al., 2013; Rathnayake et al., 2014). In addition, this coating shell is known to be a poorly ordered, amorphous, and insoluble (Rathnayake et al., 2014). Furthermore, in this study, size of three types of ZnNPs was not remarkably different in DW, a vehicle for dosing. Therefore, we hypothesized that ZnP and ZnS NPs will show lower toxicity compared to ZnO NPs due to their lower dissolution rate in the body. As expected, ZnO NPs were more rapidly ionized in artificial gastric fluid (pH 2) than ZnP and ZnS NPs. However, as unanticipated results, ZnO NPs were more easily particlized in the intestinal fluid (pH 6.8) compared to ZnP and ZnS NPs. It is noted that the additional chemicals (phosphate or sulfate) released from ZnP or ZnS NPs in gastric fluid might be suppressed by the transformation from ions to metal particles in intestinal fluid. Furthermore, we found that size of all three types of Zn-NPs in artificial gastric fluid is incredibly larger compared to them in DW against our expectation. The size of zeta potential indicates the degree of electrostatic repulsion between charged particles in dispersion. Namely, if NPs are small enough, a high zeta potential will resist aggregation (Greenwood, 2003). In this study, zeta potential of all three types of Zn-NPs in artificial gastric fluid was almost 'zero'. Therefore, we think that the high HDD values may be due to aggregation (or agglomeration) between NPs, but not growth of particle size.

Additionally, the toxicity of NPs depends primarily on the internal dose (the dose that reaches specific sites) rather than the external dose (the total dose applied via exposure route) (Oberdorster et al., 2005; Hagens et al., 2007; Braakhuis et al, 2014). Therefore, identification of the target organs in which NPs accumulate is essential for the safe and reliable use of nanotechnology in consumer products, food, medicine, and other applications. In the current study, the accumulated level in mice was generally similar between three types of Zn-NPs, and they the most distributed in the spleen and thymus. Some researchers have reported that the biological activity and biodistribution of NPs depends on secondary properties within the body as well as the primary properties of the NPs themselves, and that NPs can translocate from exposure site to other organs via various routes,

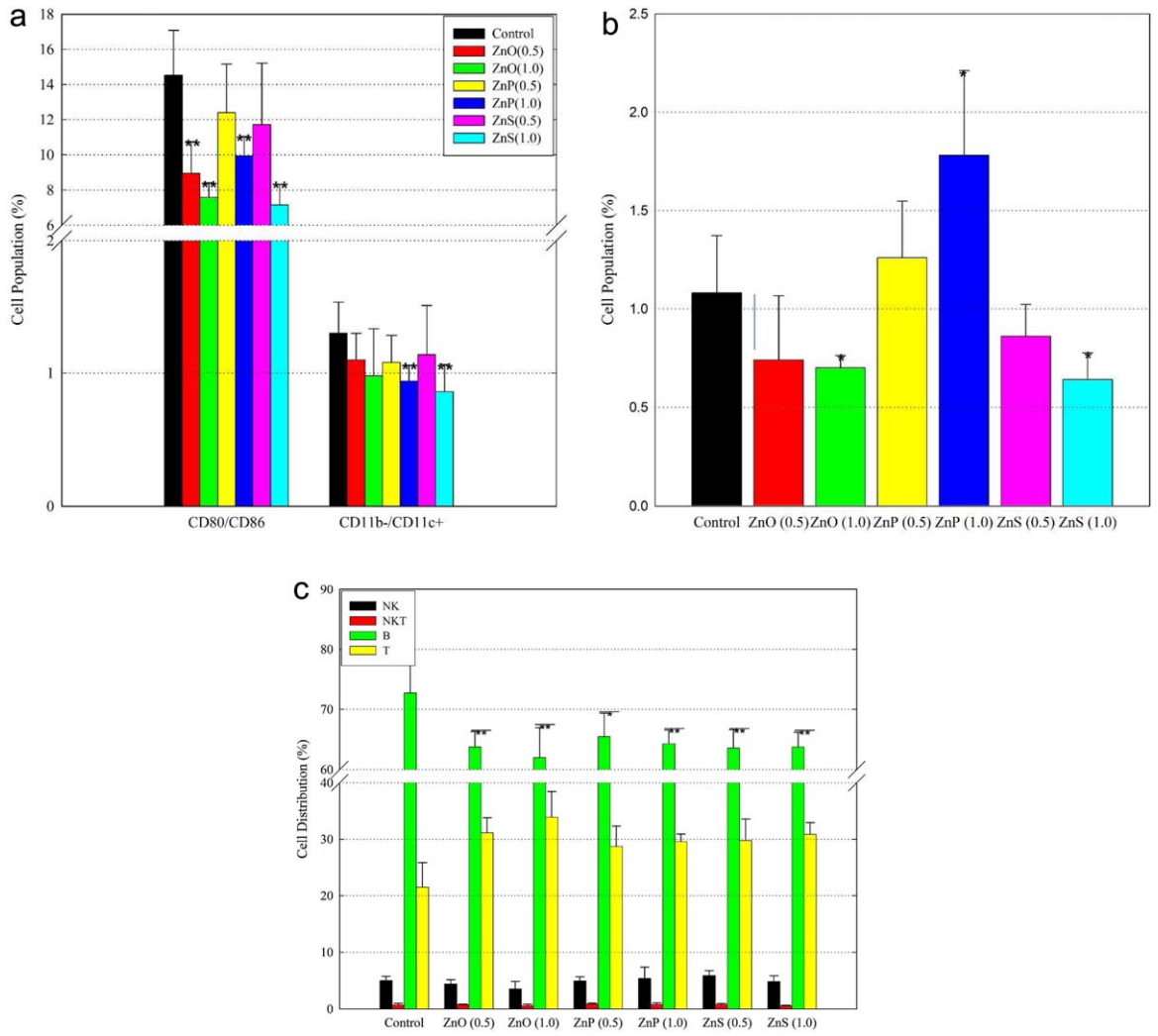

Fig. 6. Effects of Zn-NPs on expression of cell surface markers. After blocking with Fc-block antibody, splenocytes (5 samples/group) were stained in the dark with directly conjugated monoclonal antibody for 30 min at 4oC. 10,000 cells per sample were counted. *$p < 0.05$, **$p < 0.01$. (A) Expression of antigen presentation-related surface maker, 'CD11b-/CD11c+' indicates the maturated dendritic cells. (B) Expression of CXCR2 protein. (C) Cell distribution in lymphocytes of splenocytes. [Color figure can be viewed at wileyonlinelibrary.com.]

including the bloodstream and the lymphatic system, and mechanism (Hagens et al., 2007; Sayes et al., 2007; Wittmaack, 2007; Nel et al., 2009; Monopoli et al., 2012). Additionally, damaged or dead red blood cells are removed via the spleen, and some molecules filtered by the renal corpuscle can be re-absorbed by the proximal tubule and loop of Henle into the bloodstream. Furthermore, a part of NPs particlized in the intestine may be excreted outside of the body through feces. Considering that the blood shows neutral (pH 7.6–7.8), we guess that accumulation of three types of Zn-NPs in the spleen may be due to particlization of these NPs within the bloodstream (Supporting Information Fig. S2).

Some trace metal ions are essential for maintaining the normal physiological response in biological systems, but in excess, can induce toxicity by generating free radicals, such as ROS, which disrupts redox homeostasis and leads to oxidative stress (Maret, 2013; Tubek, 2007). In addition, proper electrolyte balance between the intracellular and extracellular environments is essential to maintain normal physiological function in the higher organism. However, if this balance is disrupted, it may lead to fatal health injuries in humans. For example, many biological events are regulated through kinase activity, but excessive ROS production may abnormally activate Ca2+/calmodulin-dependent protein kinase II, thereby increasing Na+ influx through voltage-gated Na+ channels. This can lead to intracellular Na+ accumulation and action potential prolongation, resulting in contractile dysfunction and irregular heartbeat in congestive heart failure patients (Kim et al., 2007; Wagner et al, 2013). Similarly, excessive ROS production may arise from excessive stimulation of the mitochondrial electron-transport chain or NAD(P)H oxidases, which leads to downstream

damage to cellular structures, including lipids and membranes, proteins, and DNA (Valko et al., 2007). In addition, metal oxide NPs, which show especially high dissolubility in biological solutions, can produce ROS that initiate redox reactions and disrupt the transfer of electrons in the body. Moreover, most metal oxide NPs are divalent in the body when dissociated, which can influence distribution of other elements and cellular processes (Cyert and Philpott, 2013; Bal et al., 2013; Park et al., 2014). Accumulated evidences show that Zn is the redox-inert transition metal that plays an essential role in diverse physiological processes, such as protein structure, catalysis, and functional regulation. However, in excess, Zn can initiate a serial toxic response by disrupting the redox balance in the body. Zn also interacts with the metabolism of other metal ions such as Cu and Fe in the body, thus overdose of Zn can cause disturbance in Fe metabolism (Blázovics et al., 2004). Similarly, increasing reports demonstrate that ZnO NPs induced oxidative stress-mediated toxic responses by disturbing both redox balance and ion balance in biological systems due to the high dissolution rate. For example, inhaled ZnO NPs damaged lung tissue through mitochondrial dysfunction, an elevated ROS production, and a disrupted signaling quiescence leading to cell death and increased expression of adaptive and inflammatory genes (Wu et al., 2013). As well, when injected ZnO NPs intraperitoneally (20–30 nm, 25 mg/kg), there are no significant effects in Zn, Na+, and K+ level in the brain, whereas Fe and Ca2+ level were clearly reduced (Amara et al., 2015). Additionally, in a previous study using human lung epithelial cells, ZnO NPs-induced cytotoicity was mitigated by supplementing the culture medium with Ca2+ (Hanagata and Morita, 2015). On the other hand, in other studies, ZnO NPs have been shown to disrupt intracellular calcium homeostasis by elevating intracellular Ca2+ level (Wang et al., 2010; Guo et al., 2013). In our previous studies, Na+ and K+ level tended to decrease in all tissues of mice injected intravenously with magnetic iron oxide NPs, whereas Ca2+ notably accumulated in these tissues (Park et al., 2016). In particular, the Ca2+ level in the brain and testes were elevated upto 13 weeks after a single injection. In the current study, we found that three types of Zn-NPs were rapidly dissociated in the artificial gastric acid, and the levels of redox reaction-related trace elements were clearly altered in all the tissues analyzed in this study. More interestingly, the homeostasis of Na+, K+, Ca2+, P, and Mg ions was remarkably disturbed in all tissues, and Na+ and K+ accumulation in the spleen and thymus in mice treated with ZnO NPs being particularly noteworthy. Moreover, compared to the control, glucose level decreased in the blood of mice treated with ZnO and ZnP NPs, and the total protein and K+ level was lower in mice treated with ZnS NPs. Considering that these ions are critical ions for normal electrophysiology and that they can be reabsorbed in the nephron, we suggest that further study to determine effects of Zn-NPs on tissue ion exchange mechanism and their clinical impact are necessary.

In the current study, three types of Zn-NPs distributed predominantly in the thymus and spleen, two major components of the lymphatic system, which are crucial for T cell selection and antibody production, respectively. Additionally, in our previous studies, suppression of antigen-presenting cell function was accompanied by a disruption in ion homeostasis following the accumulation of iron oxide NPs in the spleen (Park et al., 2016). Similarly, it is known that Zn can influence all aspects of innate and adaptive immunity (Haase and Rink, 2014). Moreover, although it is still under debate, the effects of ZnO NPs on the immune system have been raised in some studies (Kim et al., 2014a; Roy et al., 2014). For example, topical application of ZnO NPs reduced local skin inflammation but induced systemic production of IgE antibodies in the atopic dermatitis model (Ilves et al., 2014). Additionally, ZnO NPs (750 mg/kg/day) administered orally for 14 days suppressed innate immunity without an effect on the T cell-mediated immune response, the ratio of CD4+/CD8+, subtypes of T cells, was slightly reduced, and serum levels of pro-, anti-, and Th1 type-inflammatory cytokines were significantly inhibited in mice exposed to ZnO NPs compared to the control (Kim et al., 2014b). In the current study, three types of ZnNPs enhanced T cell distribution in lymphocytes and suppressed the function of antigen-presenting cells. Additionally, ZnO and ZnP NPs, but not ZnS NPs, tended to increase the distribution of cytotoxic T cells compared to that of helper T cells (data not shown). The Na+/H+ exchanger (NHE) is involved in pH regulation and removal of intracellular acid, exchanging a proton for an extracellular Na+. A specific isoform of NHE, NHE-1, but not other isoforms, plays a crucial role in extruding H+ and regulating pH in the immune system. NHE-1 also affects Ca2+ homeostasis in microglia and contributes to the increase of Ca2+ by stimulating the Na+/Ca2+ exchanger, thus regulating immune cell function (Shi et al., 2013). Additionally, Ca2+/calmodulin-dependent protein kinase II is necessary for T cell selection and CD8+ T cell activation (Lin et al., 2005; Boubali et al., 2012). Thus, we hypothesize that alterations in immune regulation following the bioaccumulation of three types of Zn-NPs may be attributable, at least in part, to the altered tissue ion levels.

Taken together, we conclude that Zn-NPs may induce adverse effects on human health by disrupting homeostasis of trace elements and ions in the tissues. In addition, coating ZnO NPs with phosphate and sulfide may not significantly alleviate the toxicity due to the higher particlization rate of ZnO NPs in the intestine, at least in part.

REFERENCES

Akhtar MJ, Ahamed M, Kumar S, Khan MM, Ahmad J, Alrokayan SA. 2012. Zinc oxide nanoparticles selectively

induce apoptosis in human cancer cells through reactive oxygen species. Int J Nanomedicine 7:845–857.

Amara S, Slama IB, Omri K, Ghoul JE, Mir LE, Rhouma KB, Abdelmelek H, Sakly M. 2015. Effects of nanoparticle zinc oxide on emotional behavior and trace elements homeostasis in rat. Brain 31:1202–1209.

Bal, W., Sokolowska, M., Kurowska, E., Faller, P., 2013. Binding of transition metal ions to albumin: sites, affinities and rates. Biochim. Biophys. Acta 1830:5444–5455.

Blázovics A, Szentmihályi K, Prónai L, Hagymási K, Lugasi A, Kovács A, Fehér J. 2004. Redox homeostasis in inflammatory bowel diseases. Orv Hetil 145:1459–1466.

Boubali S, Liopeta K, Virgilio L, Thyphronitis G, Mavrothalassitis G, Dimitracopoulos G, Paliogianni F. 2012. Calcium/calmodulin-dependent protein kinase II regulates IL-10 production by human T lymphocytes: A distinct target in the calcium dependent pathway. Mol Immunol 52:51–60.

Braakhuis HM, Park MV, Gosens I, De Jong WH, Cassee FR. 2014. Physicohemical characteristics of nanomaterials that affect pulmonary inflammation. Part Fibre Toxicol 11;18.

Choi SJ, Choy JH. 2014. Biokinetics of zinc oxide nanoparticles: Toxicolkinetics, biological fates, and protein interaction. Int J Nanomedicine 9:261–269.

Cyert MS, Philpott CC. 2013. Regulation of cation balance in Saccharomyces cerevisiae. 193:677-713.

Greenwood R. 2003. Review of the measurement of zeta potentials in concentrated aqueous suspensions using electroacoustics. Adv Colloid Interfce Sci 106:55–81.

Guo D, Bi H, Wang D, Wu Q. 2013. Zinc oxide nanoparticles decrease the expression and activity of plasma membrane calcium ATPase, disrupt the intracellular calcium homeostasis in rat retinal ganglion cells. Int J Biochem Cell Biol 45:1849–1859.

Hagens WI, Oomen AG, de Jong WH, Cassee FR, Sips AJ. 2007. What do we (need to) know about the kinetic properties of nanoparticles in the body? Regul Toxicol Pharmacol 49:217–229.

Hanagata N, Morita H. 2015. Calcium ions rescue human lung epithelial cells from the toxicity of zinc oxide nanoparticles. J Toxicol Sci 40:625–635.

Haase H, Rink L. 2014. Zinc signals and immune function. Biofactors 40:27–40.

Horev-Azaria L, Kirkpatrick CJ, Korenstein R, Marche PN, Maimon O, Ponti J, Romano R, Rossi F, Golla-Schindler U, Sommer D, Uboldi C, Unger RE, Villiers C. 2011. Predictive toxicology of cobalt nanoparticles and ions: comparative in vitro study of different cellular models using methods of knowledge discovery from data. Toxicol Sci 122:489–501.

Ilves M, Palomäki J, Vippola M, Lehto M, Savolainen K, Savinko T, Alenius H. 2014. Topically applied ZnO nanoparticles suppress allergen induced skin inflammation but induce vigorous in the atopic dermatitis mouse model. Part Fibre Toxicol 11:38.

Jiang C, Aiken GR, Hsu-Kim H. Effects of natural organic matter properties on the dissolution kinetics of zinc oxide nanoparticles. Environ Sci Technol 49:11476–11484.

Kim CS, Davidoff AJ, Maki TM, Doye AA, Gwathmey JK. 2000. Intracellular calcium and the relationship to contractility in an avian model of heart failure. J Comp Physiol B 170:295–306.

Kim Y, Kim C, Choi I, Rengaraj S, Yi J. 2004. Arsenic removal using mesoporous alumina prepared via a templating method. Environ Sci Technol 38:924–931.

Kim YH, Fazlollahi F, Kennedy IM, Yacobi NR, Hamm-Alvarez SF, Borok Z, Kim KJ, Crandall ED. 2010. Alveolar epithelial cell injury due to zinc oxide nanoparticle exposure. Am J Respir Crit Care Med 182:1398–1409.

Kim CS, Nguyen HD, Ignacio RM, Kim JH, Cho HC, Maeng EH, Kim YR, Kim MK, Park BK, Kim SK. 2014a. Immunotoxicity of zinc oxide nanoparticles with different size and electrostatic charge. Int J Nanomed 9:195–205.

Kim MH, Seo JH, Kim HM, Jeong HJ. 2014b. Zinc oxide nanoparticles, a novel candidate for the treatment of allergic inflammatory diseases. Eur J Pharmacol 738:31–39.

Kwok KW, Dong W, Marinakos SM, Liu J, Chilkoti A, Wiesner MR, chernick M, Hinton DE. 2016. Silver nanoparticle toxicity is related to coating materials and disruption of sodium concentration regulation. Nanotoxicology Epub ahead of print.

Li CH, Shen CC, Cheng YW, Huang SH, Wu CC, Kao CC, Liao JW, Kang JJ. 2012. Organ biodistribution, clearance, and genotoxicity of orally administered zinc oxide nanoparticles in mice. Nanotoxicology 6:746–756.

Lin MY, Zal T, Ch'en IL, Gascoigne NR, Hedrick SM. 2005. A pivotal role for the multifunctional calcium/calmodulin-dependent protein kinase II in T cells: From activation to unresponsiveness. J Immunol 174:5583–5592.

Luo M, Shen C, Feltis BN, Martin LL, Hughes AE, Wright PF, Turney TW. 2014. Reducing ZnO nanoparticle cytotoxicity by surface modification. Nanoscale 6:5791–5798.

Ma R, Levard C, Michel FM, Brown GE Jr, Lowry GV. 2013. Sulfidation mechanism for zinc oxide nanoparticles and the effect of sulfidation on their solubility. Environ Sci Technol 47:2527–2534.

Maret W. 2013. Zinc and human disease. Met Ions Life Sci 13: 389–414.

Marques MRC, Loebenberg R, Almukainzi M. 2011. Simulated biological fluids with possible application in dissolution testing. Dissolut Technol 8:15–28.

Monopoli MP, Aberg C, Salvati A, Dawson KA. 2012. Biomolecular coronas provide the biological identity of nanosized materials. Nat Nanotechnol 7:779–786.

Nel AE, Mädler L, Velegol D, Xia T, Hoek EM, Somasundaran P, Klaessig F, Castranova V, Thompson M. 2009. Nat Mater 8: 543–557.

Nohynek GJ, Antignac E, Re T, Toutain H. 2010. Safety assessment of personal care products/cosmetics and their ingredients. Toxicol Appl Pharmacol 243:239–259.

Oberdörster G, Oberdörster E, Oberdörster J. 2005. Nanotoxicology: an emerging discipline evolving from studies of ultrafine particles. Environ Health Perspect 113:823–839.

Ortega R, Bresson C, Darolles C, Gautier C, Roudeau S, Perrin L, Janin M, Floriani M, Aloin V, Carmona A, Malard V. 2014. Low-solubility particles and a Trojan-horse type mechanism of

toxicity: The case of cobalt oxide on human lung cells. Part Fibre Toxicol 11:14-

Park EJ, Yi J, Kim Y, Choi K, Park K. 2010. Silver nanoparticles induce cytotoxicity by a Trojan-horse type mechanism. Toxicol in Vitro 24:872–878.

Park EJ, Lee GH, Yoon C, Kang MS, Kim SN, Cho MH, Kim JH, Kim DW. 2014. Time-dependent bioaccumulation of distinct rod-type TiO2 nanoparticles: Comparison by crystalline phase. J Appl Toxicol 34:1265–1270.

Park EJ, Kim SW, Yoon C, Kim Y, Kim JS. 2016. Disturbance of ion environment and immune regulation following biodistribution of magnetic iron oxide nanoparticles injected intravenously. Toxicol Lett 243:67–77.

Rathnayake S, Unrine JM, Judy J, Miller AF, Rao W, Bertsch PM. 2014. Multitechnique investigation of the pH dependence of phosphate induced transformations of ZnO nanoparticles. Environ Sci Technol 48:4757–4764.

Roy R, Kumar S, Verma AK, Sharma A, Chaudhari BP, Tripathi A, Das M, Dwivedi PD. 2014. Zinc oxide nanoparticles provide an adjuvant effect to ovalbumin via a Th2 response in Balb/c mice. Int Immunol 26:159–172.

Sabella S, Carney RP, Brunetti V, Malvindi MA, Al-Juffali N, Vecchio G, Janes SM, Bakr OM, Cingolani R, Stellacci F, Pompa PP. 2014. A general mechanism for intracellular toxicity of metal-containing nanoparticles. Nanoscale 6:7052–7061.

Sayes CM, Reed KL, Warheit DB. 2007. Assessing toxicity of fine and nanoparticles: Comparing in vitro measurements to in vivo pulmonary toxicity profiles. Toxicol Sci 97:163–180.

Sensi SL, Jeng JM. 2004. Rethinking the excitotoxic ionic milieu: The emerging role of Zn(2+) in ischemic neuronal injury. Curr Mol Med 4:87–111.

Shi Y, Kim D, Caldwell M, Sun D. 2013. The role of Na(+)/H(+) exchanger isoform 1 in inflammatory responses: Maintaining H(+) homeostasis of immune cells. Adv Exp Med Biol 961:411–418.

Song W, Zhang J, Guo J, Zhang J, Ding F, Li L, Sun Z. 2010. Role of the dissolved zinc ion and reactive oxygen species in cytotoxicity of ZnO nanoparticles. Toxicol Lett 199:389–397.

Tubek S. 2007. Zinc supplementation or regulation of its homeostasis: Advantages and threats. Biol Trace Elem Res 119:1–9.

Valko M, Leibfritz D, Moncol J, Cronin MT, Mazur M, Telser J. 2007. Free radicals and antioxidants in normal physiological functions and human disease. Int J Biochem Cell Biol 39:44–84.

Vandebriel RJ, De Jong WH. 2012. A review of mammalian toxicity of ZnO nanoparticles. Nanotechnol Sci Appl 5:61–71.

Wittmaack K. 2007. In search of the most relevant parameter for quantifying lung inflammatory response to nanoparticle exposure: particle number, surface area, or what? Environ Health Perspect 115:187–194.

Wagner S, Rokita AG, Anderson ME, Maier LS. 2013. Redox regulation of sodium and calcium handling. Antioxid Redox Signal 18:1063–1077.

Wang HJ, Growcock AC, Tang TH, O'Hara J, Huang YW, Aronstam RS. 2010. Zinc oxide nanoparticle disruption of store-operated calcium entry in a muscarinic receptor signaling pathway. Toxicol in Vitro 24:1953–1961.

Wang X, Ji Z, Chang CH, Zhang H, Wang M, Liao YP, Lin S, Meng H, Li R, Sun B, Winkle LV, Pinkerton KE, Zink JI, Xia T, Nel AE. 2014. Use of coated silver nanoparticles to understand the relationship of particle dissolution and bioavailability to cell and lung toxicological potential. Small 10:385–398.

Wu W, Bromberg PA, Samet JM. 2013. Zinc ions as effectors of environmental oxidative lung injury. Free Radic Biol Med 65: 57–69.

Zhang W, Yang L, Kuang H, Yang P, Aguilar ZP, Wang A, Fu F, Xu H. 2016. Acute toxicity of quantum dots on late pregnancy mice: Effects of nanoscale size and surface coating. J Hazard Mater 318:61–69.